Particle backgrounds for satellites in an inclined orbit

Kishalay De

August 10, 2020

1 Introduction

The aim of this article is to discuss the particle background for low Earth orbit (LEO) X-ray satellites in an inclined orbit. Example missions are the Rossi X-ray Timing Explorer (RXTE; altitude $\approx$ 580 km and inclination $\approx$ 23 degrees), the Hard X-ray Modulation Telescope (HXMT; altitude $\approx$ 550 km and inclination $\approx$ 43 degrees) and the *Suzaku* mission (altitude $\approx$ 550 km and inclination $\approx$ 31 degrees). Specific aspects relevant to inclined orbits are discussed in this article, as general properties of the particle background are discussed in other articles.

2 Particle background in varying geomagnetic locations

For LEO satellites, the particle background is a strong function of the geographical position due to the varying strength of the Earth's geomagnetic field, which shields the satellites from incoming cosmic ray particles. The relevant background is primarily that of cosmic ray protons, electrons and positrons incident on the Earth's magnetosphere. While the incident cosmic ray spectrum is well characterized by other missions (and summarized in other articles in this series), I will discuss here specific aspects important for inclined LEOs. For an incident cosmic ray flux $F(E)$, the geomagnetic field modifies the flux received at the satellite $F_s(E)$ by the geomagnetic cut-off function $C(R, h, \theta_M)$, i.e.

$$F_s(E) = F(E)C(R, h, \theta_M) \tag{1}$$

where h is the orbit height and θ_M is the geomagnetic latitude. The cut-off function is approximated as (Mizuno et al. 2012)

$$C(R, h, \theta_M) = \frac{1}{1 + (R/R_{cut})^{-r}} \tag{2}$$

where the cut-off rigidity is given by the Stromer equation (Smart et al. 2004)

$$R_{cut} = 14.5 \times \left(1 + \frac{h}{R_E}\right)^{-2} \cos^4 \theta_M \mathrm{GV} \tag{3}$$

where $R_E = 6371$ km is the Earth radius and the exponent $r = 12$ for protons and $r = 6$ for electrons and positrons. From equations 2 and 3, one sees that cut-off function increases

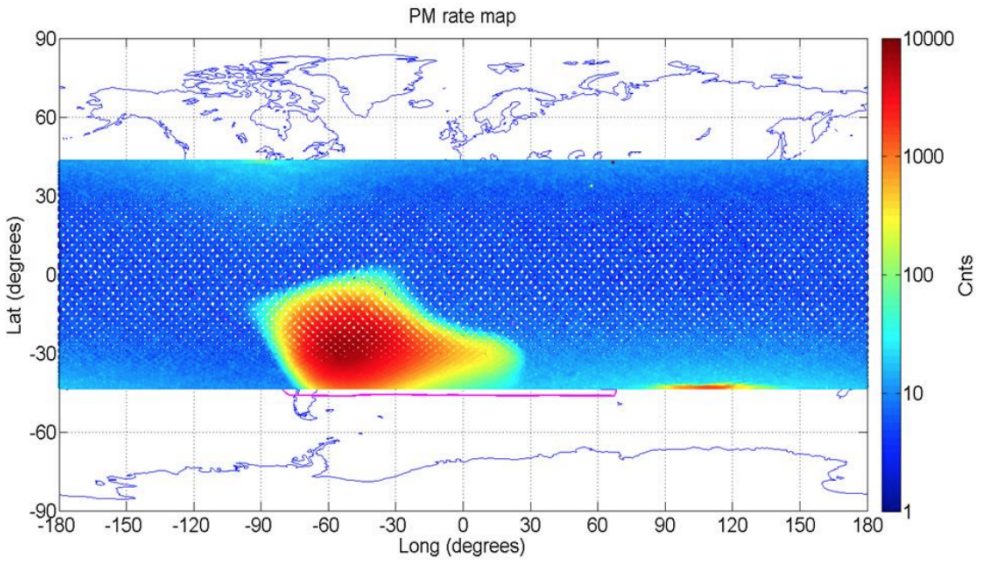

Figure 1: Observed particle background by the particle monitor on board HXMT (from Zhang et al. 2019).

rapidly for higher geomagnetic latitudes near the poles and so does the incident particle background.

However, equation 3 is not strictly true due to the non-concentricity of the Earth's magnetosphere and the rotation axis, i.e., for a given height above the Earth's surface all directions are not equal in geomagnetic latitude. The most prominent example of the deviation of R_{cut} from a simple cosine law is the South Atlantic Anomaly (SAA) over the northern South America and the south Atlantic ocean. Here, the Earth's magnetic fields is weakest compared to an idealized dipole, leading to a lower height of the Van-Allen radiation belt which traps particles from the solar wind. Thus, satellites passing near or through the SAA (particularly problematic for **all** satellites on an inclined orbit) are subjected to substantially higher particle backgrounds, and often forced to shut down their instruments for safety. Figure 1 shows the observed particle background as a function of geographical location as observed by the particle monitor on board the HXMT satellite. Note the high count rates encountered near the SAA, as well as the increasing background near geomagnetic poles (equation 3).

Instead, a common way to characterize the particle attenuation caused by the magnetosphere is with maps of the the geomagnetic cut-off rigidity R_{cut} (which has units of GV) as a function of latitude and longitude. Larger R_{cut} corresponds to more attenuation of the incident particle flux and hence lower particle background. Figure 2 shows a typical variation of the particle background as a fuction of the R_{cut} (abbreviated as COR in the plot), as observed by the Medium Energy Telescope on board HXMT.

Specifically, it is worth noting that while the intensity of the background varies substantially with changing R_{cut} in the Earth's geomagnetic field, its spectrum has been observed to be very stable, i.e., the particle background only changes in an achromatic flux scaling. Figure 3 shows the observed spectrum of the particle background for different R_{cut}/COR, as observed by the low energy telescope onboard HXMT, demonstrating the stable spectrum

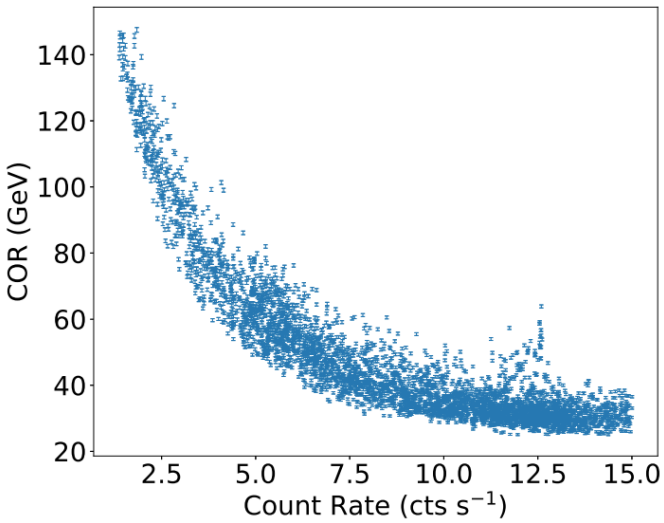

Figure 2: Particle count rate as a function of the cut-off rigidity R_{cut} ($= COR$) as observed by the Medium Energy Telescope on board HXMT (from Guo et al. 2020).

of the particle background.

3 Particle backgrounds due to induced radioactivity

Passage through the SAA creates another sources of background specific to highly inclined orbits, caused by induced radioactivity from activated isotopes. As the satellite passes through the SAA, high intensity proton flux from 100 keV to 400 keV activates radio nuclides in the satellite material, which then subsequently decay over timescales of the radioactive half-life of the nuclide. Figure 4 shows the decay in the background count rate as a function of time after SAA passage, demonstrating that the increased background persists for several minutes after the SAA passage but is then dominated by the background from the isotopes with the longest half-lives. Over the initial period of commissioning, the general particle background of the satellites increase and stabilize with time due to repeated activattion of the longest lived isotopes.

References

Campana, R., Feroci, M., Del Monte, E. et al. Background simulations for the Large Area Detector onboard LOFT. Exp Astron 36, 451–477 (2013).

Guo, C.-C., Liao, J.-Y., Zhang, S., et al. 2020, Journal of High Energy Astrophysics, 27, 44

Liao, J.-Y., Zhang, S., Chen, Y., et al. 2020, Journal of High Energy Astrophysics, 27, 24

Xie, F., Zhang, J., Song, L.-M., et al. 2015, Ap&SS, 360, 13

Zhang, S., Zhang, S. N., Lu, F. J., et al. 2018, Proc. SPIE, 10699, 106991U

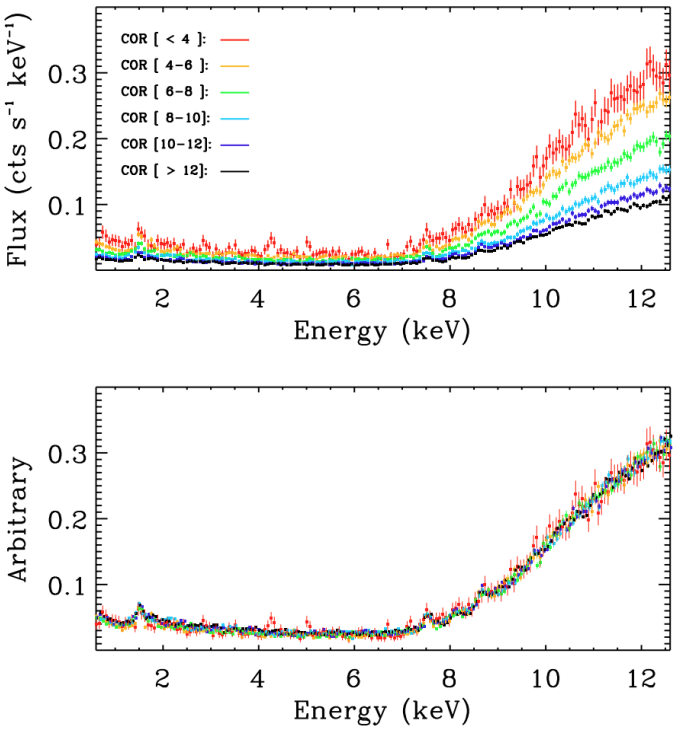

Figure 3: (Top) The observed spectrum of the particle background as a function of the cut-off rigidity COR, showing the increasing background levels with decreasing COR. (Bottom) Normalized spectrum of the particle background for different COR demonstrating the stability of the spectrum for different background rates (from Liao et al. 2020).

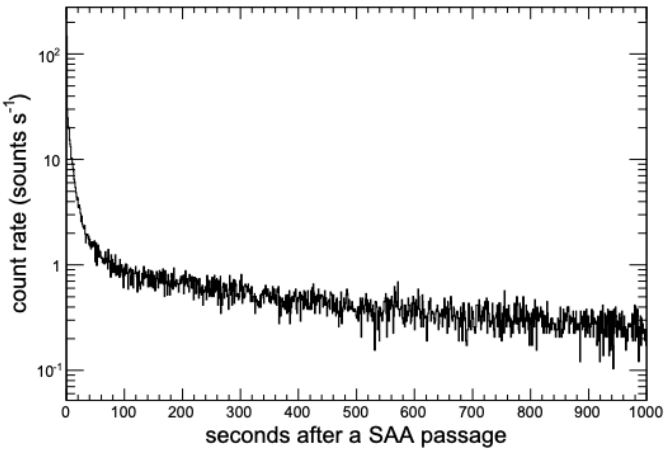

Figure 4: Background count rate as a function of time after passage through SAA, showing the rapid decay in background following SAA passage, simulated for the high energy telescope on board HXMT (from Xie et al. 2015).